OPTICAL POLARIZATION PROPERTIES OF THE DIFFRACTION SPECTRA FROM SINGLE FIBERS OF SKELETAL MUSCLE

Y. YEH AND B. G. PINSKY
Department of Applied Science, University of California, Davis, California 95616

ABSTRACT The diffraction spectra of laser light from single fibers of skeletal muscle exhibit a large degree of optical depolarization. When the linearly polarized incident laser source is oriented at polarization angles between $0 < \Theta < \pi/2$ rad with respect to the fiber axis, the diffracted light is elliptically polarized. These results show that the phase angle of the ellipse rotates by as much as 20° when the fiber is stretched from 2.4 to 3.8 μm. To further ascertain that the observed phenomenon is diffraction related, an experiment monitoring the spectra of scattered light in between diffraction orders showed this signal to be significantly more linearly polarized. These results suggest that the degree of elliptical polarization of the diffraction spectra is a sensitive probe of A-band dynamics, including changes of the anisotropic S-2 elements.

INTRODUCTION

A fundamental question in the structural and functional determination of the mechanism of skeletal muscle contraction is the role and the action played by the S-2 part of the myosin molecule. The S-2 moiety forms the linkage between the ATPase portions (S-1 subfragments) and the rigid section called light meromyosin (LMM). The latter aggregates to form the stalk of the thick filament. LMM and S-2 together show >95% α-helical composition (1). Besides serving as this necessary mechanical link, it has been suggested that the S-2 element provides tension (2), produces restoring force by its elastic properties (3), or supplies necessary bending motion during tension generation (4).

Recent depolarized laser-scattering studies on isolated myosin rods (LMM + S-2) have shown that a flexible joint exists between these two α-helical elements (5). Probing of the dynamics of S-2 in situ in a single fiber is necessarily more complicated. X-ray diffraction studies have shown that an increase in the intensity ratio of the (1,1) to (1,0) equatorial lines takes place during tetanic contraction (6,7). This shift in intensity has been interpreted as material movement from the thick filament region to the actin filament region when contraction takes place. From this result, one may infer that S-2 must have executed some motion to allow the mass (S-1 moities) to move towards the actin filaments during contraction.

A second probe of possible dynamic changes of the S-2 element comes from optical birefringence studies. In the work of Taylor (8), changes in optical phase shift of the transmitted visible light are detected between a fiber in its resting state and when it is actively contracting. This change is interpreted as possible positional changes of the S-2 element taking place during contraction. However, there are two major difficulties associated with birefringence experiments. First, all optically anisotropic elements in the fiber (9) as well as periodically arranged isotropic elements (form birefringence) are detected along with the contribution from the element of interest. Second, the strong noninteractive transmitted light precludes the possibility of accurately measuring simultaneously both the optical phase shift and the degree of ellipticity, both of which are needed for complete characterization of the elliptically polarized light (10). Indeed all birefringence work is conducted by using a phase compensator, which does not measure the ellipticity of the transmitted light. The present work develops a new technique of optical measurement which will provide a complete description of the light that has interacted with the fiber and that is also selective against all nonsarcomere related contributions.

It is well known that optical diffraction technique provides spatially specific information on the diffracting elements (11). In this study, we have measured changes of optical depolarization within the diffraction peaks. Information obtained from these studies aids in distinguishing between orientational or attitudinal changes and intrinsic conformational changes that may occur within the A-band regions.

This work is preliminary because only the passive stretch experiment has been conducted. On the other hand, such a study provides a baseline for a situation where intrinsic conformation-induced anisotropy changes may be assumed absent. We show here that the ratio of optical polarizabili-

Address all reprint requests to Y. Yeh.

ties remains constant, whereas a definite decrease in phase shift (~ 20%) is detected upon passive stretch from a resting length of 2.4 μm to beyond overlap at 3.8 μm. We have tentatively attributed this change in phase shift to an increase in the amount of orientational flexibility at the LMM–S-2 joint when the thick filament is pulled away from overlap.

THEORY

When light wave of a definite wavelength and polarization interacts with a medium, changes in wavelength or polarization reflect the interaction mechanism, whether one is detecting the transmission, reflection, scattering, or diffraction of light. For nonwavelength changing processes, the general Mueller matrix method can be used to describe the development of the light field from one polarization and intensity state to another as it interacts with a material element (12). The vector representation for the state of the light is called a Stoke's vector, $\mathbf{V} = (I_0, Q_0, U_0, V_0)$. This four-component vector denotes the intensity, the horizontal and 45° linear polarization preference, and the sense of optical rotation, respectively. When light described by $\mathbf{V}_0 = (I_0, Q_0, U_0, V_0)$ interacts with an element, the interaction may be represented by a transformation that takes the $\mathbf{V}_1$ via the matrix operation

$$\mathbf{V}_1 = \bar{\bar{M}} \cdot \mathbf{V}_0, \tag{1}$$

where $\bar{\bar{M}}$ is a 4 × 4 matrix representing all of the transformation properties of light. Successive interactions may be similarly represented

$$\mathbf{V}_n = \bar{\bar{M}}_n \cdot \bar{\bar{M}}_{n-1} \cdot \ldots \cdot \bar{\bar{M}}_2 \cdot \bar{\bar{M}}_1 \mathbf{V}_0. \tag{2}$$

If all of the $\bar{\bar{M}}$ matrices were known, then $\mathbf{V}_n$ is totally characterized. If, however, $\mathbf{V}_n$ can be determined experimentally, along with all of the $\bar{\bar{M}}$ matrices except one, then that unknown matrix can be determined completely. In the single fiber diffraction experiment designed to be sensitive to the changes of the polarization state, the unknown matrix represents the properties of the single fiber of muscle cell that alters the light properties of the V vector.

In the experiments described below, $\mathbf{V}_0$, the incident light source and $\mathbf{V}_n$, the final diffracted and processed light signal, are both measured quantities. All optical elements used to alter the optical signal also have well-characterized $\bar{\bar{M}}$ matrices. We are thus left with the determination of the matrix element that best characterizes the single fiber. To determine this fiber-specific matrix, we begin by examining the diffraction geometry. By considering the fiber as a cylinder lying along the y-axis (Fig. 1), we impose the incident light field with polarization in the x-y plane propagating along the z-axis. Thus the incident electric-field vector is given by $\mathbf{E}_0(\mathbf{k}_0, t)$, where $|k_0| = 2\pi/\lambda$; λ is the wavelength of light in the medium. Detection is in the plane of y-z at an angle of Θ_D, where the new light polarization vector, $\mathbf{k}_s$, is directed along z'. We assume a

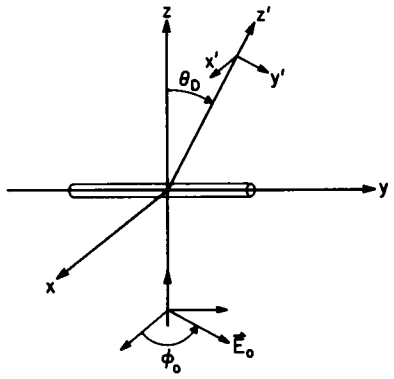

FIGURE 1 Coordinate representation of the experiment. The incident light is directed along z-axis with linear polarization at an angle ϕ_o in the x-y plane. The fiber lies on the y-axis. Detection is along the z' axis, which is tilted at the diffraction angle, Θ_D.

model of the fiber where the anisotropic fiber provides a polarizability tensor of the form

$$\bar{\alpha} = \begin{bmatrix} \alpha_\perp & 0 & 0 \\ 0 & \alpha_\parallel e^{-i\delta} & 0 \\ 0 & 0 & \alpha_\perp \end{bmatrix}, \tag{3}$$

where the fiber axis y is assumed to have different complex polarizability relative to that of the transverse directions (x and z). Here, $\alpha_\perp$ and $\alpha_\parallel$ are the polarizability magnitudes transverse to and along the fiber axis, respectively. δ is the net optical-phase difference between the slower longitudinal and the faster transverse axes. Using the dipole-scattering approximation (13), $\mathbf{E}_{sc} \propto \hat{\mathbf{k}}_s \times (\hat{\mathbf{k}}_s \times \bar{\bar{\alpha}} \cdot \mathbf{E}_o)$, one finds that the scattered field directed along z' is given by

$$(\mathbf{E}_{sc})_{z'} \propto \begin{bmatrix} \alpha_\perp e^{i\delta} \cos\phi_o \\ \alpha_\parallel \cos\Theta_D \sin\phi_o \\ 0 \end{bmatrix}, \tag{4}$$

where ϕ_o is the orientational angle of the incident linear polarization with respect to the fiber. The fundamental definition of the elements of a Stoke's vector is given by (12)

$$\mathbf{V} = \begin{bmatrix} I \\ Q \\ U \\ V \end{bmatrix} = \begin{bmatrix} \langle E_x^* E_x + E_y^* E_y \rangle \\ \langle E_x^* E_x - E_y^* E_y \rangle \\ \langle E_x^* E_y + E_y^* E_x \rangle \\ -i\langle E_x^* E_y - E_y^* E_x \rangle \end{bmatrix}, \tag{5}$$

where E_x and E_y are the general transverse field components; $\langle \ldots \rangle$ denotes long time average or ensemble average for ergodic systems. For the specific system under consideration, the incident electric-field leads to a Stoke's

vector given by

$$\mathbf{V}_0 = \begin{bmatrix} 1 \\ \cos^2\phi_o - \sin^2\phi_o \\ 2\cos\phi_o \sin\phi_o \\ 0 \end{bmatrix}. \quad (6)$$

The diffracted light has the following Stoke's vector

$$\mathbf{V}_M = \begin{bmatrix} |\alpha_\perp|^2 \cos^2\phi_o + |\alpha_\parallel|^2 \sin^2\phi_o \cos^2\Theta_D \\ |\alpha_\perp|^2 \cos^2\phi_o - \alpha_\parallel^2 \sin^2\phi_o \cos^2\Theta_D \\ 2\alpha_\perp\alpha_\parallel \cos\Theta_D \cos\phi_o \sin\phi_o \cos\delta \\ -2\alpha_\perp\alpha_\parallel \cos\Theta_D \cos\phi_o \sin\phi_o \sin\delta \end{bmatrix} \quad (7)$$

using the relationship $\mathbf{V}_M = \bar{\bar{M}}_M \cdot \mathbf{V}_0$, one obtains the elements of the interaction matrix $\bar{\bar{M}}_M$. For the specific case of $\phi_o = +\pi/4$ rad,

$$\bar{\bar{M}}_M = \begin{bmatrix} A & B & O & O \\ B & A & O & O \\ O & O & C & -D \\ O & O & D & C \end{bmatrix}, \quad (8)$$

where

$$A = \tfrac{1}{2}(\alpha_\perp^2 + \alpha_\parallel^2 \cos^2\Theta_D) \quad (9a)$$

$$B = \tfrac{1}{2}(\alpha_\perp^2 - \alpha_\parallel^2 \cos^2\Theta_D) \quad (9b)$$

$$C = +\alpha_\perp \alpha_\parallel \cos\Theta_D \cos\delta \quad (9c)$$

$$D = -\alpha_\perp \alpha_\parallel \cos\Theta_D \sin\delta. \quad (9d)$$

The detected Stoke's vector is given by

$$\mathbf{V}_D = \bar{\bar{M}}_D \cdot \bar{\bar{M}}_M \cdot \mathbf{V}_0 = \bar{\bar{M}}_D \cdot \mathbf{V}_M, \quad (10)$$

where $\mathbf{V}_0$, $\mathbf{V}_M$, and $\bar{\bar{M}}_M$ are given by Eqs. 6–9. The matrix $\bar{\bar{M}}_D$ contains all of the detection optics components; and $\mathbf{V}_D$ is the final Stoke's vector. Using an intensity sensitive device, such as a photomultiplier tube, only the first element, I_D of $\mathbf{V}_D$, is measured. The M_D in this experiment represents the combination of a $\lambda/4$ wave plate that rotates through an angle Θ from 0° to 360°, and a polarizer that is set to pass only that component of electric-field vector perpendicular to the fiber axis. Writing $\mathbf{V}_M = (I_M, Q_M, U_M, V_M)$, we obtain

$$I_D = \frac{1}{2}(I_M + Q_M \cos^2 2\Theta + U_M \cos 2\Theta \sin 2\Theta - V_M \sin 2\Theta). \quad (11)$$

When $\mathbf{V}_M$ has been determined experimentally, the relationship of Eq. 9 can be used to determine the relevant fiber parameters, δ_M, $\alpha_\perp$, and $\alpha_\parallel$

$$\tan\delta_M = \frac{(-D)}{C} \quad (12a)$$

$$\alpha_\parallel = \left(\frac{A-B}{2}\right)^{1/2} \frac{1}{\cos\Theta_D} \quad (12b)$$

$$\alpha_\parallel = \left(\frac{A+B}{2}\right)^{1/2}. \quad (12c)$$

From the last two equations, we can obtain the ratio

$$\tan\alpha_M \equiv \frac{\alpha_\parallel}{\alpha_\perp}\cos\Theta_D. \quad (13)$$

Furthermore, the relationship between δ_M and α_M or $\alpha_\perp$ and $\alpha_\parallel$ is given by the optical path-length-induced phase-shift difference

$$\delta_M = \frac{2\pi}{\lambda_0} d\,(\alpha_\perp^{1/2} - \alpha_\parallel^{1/2}), \quad (14)$$

where d is the material distance traversed by the light. Thus through the interaction of light with the fiber, a full characterization of $\mathbf{V}_M$ allows simultaneous determination of δ_M and α_M, the fiber contribution to the phase shift and ellipticity, respectively.[1]

EXPERIMENTAL METHODS AND PROCEDURE

Incident on the muscle fiber is a beam of highly linearly polarized light, oriented at 45° (Fig. 2) relative to the muscle fiber axis. This is accomplished by passing the laser beam from a He-Ne laser (145-P; Spectra-Physics Inc., Mountain View, CA) through a glass prism polarizer (extinction coefficient = 1:10^4). The polarization is then rotated relative to the fiber by a $\lambda/2$-wave plate (Melles Griot, Irvine, CA). The detection optics, a rotating quarter-wave plate, a stationary glass prism polarizer, fiber optic light pipe, and photomultiplier (PM) tube are mounted on a rotating arm. The axis of rotation for this arm is centered at the fiber level and in the plane of the axis of the fiber. Both the arm and quarter-wave plate are rotated by a stepping motor and worm gear arrangement. The accuracy of rotational repeatability of the arm and the quarter-wave plate are 0.01° and 0.17°, respectively. The accuracy of the arm's rotation is checked against a known transmission grating and the accuracy of the quarter-wave plate rotation against a known retardation plate. The arm can be held in position in the scattered field, allowing for analysis of the polarization of the scattered field by rotating the quarter-wave plate. The diffracted light, after passing through the detector optics, is collected by a 1/4-in diam light pipe and transmitted to a PM tube (EMI 9558B; EMI Gencom, Inc., Plainview, NY). Because the PM tube only detects intensity, the final result is as given by Eq. 11, where Θ corresponds to the angular rotation of the quarter-wave plate and I is the intensity at the PM tube. The intensity is then collected and displayed in real time on an LSI 11/2 microcomputer (LSI Computer Systems, Inc., Melville, NY). The coefficients of $\mathbf{V}_M$ are then determined by a multiple linear regression program (14) on Eq. 11. These parameters, combined in accordance with Eqs. 11–14, determine the polarization properties as described in the Theory section.

The single muscle and its tendons are dissected from the dorsal head of the semitendinosus muscle of frogs (*Rana pipiens*). The muscle fiber is dissected in cold Ringer's solution (5°C) by using forceps and ophthalmic scissors. The tendons are tied with 6-0 gauge silk suture. When the fiber is

[1]The present formulation of general elliptically polarized light can be related to the more conventional representation as that found in Mathieu (10). A discussion of the ellipsometry measurement technique may be found in Azzam and Bashara (22).

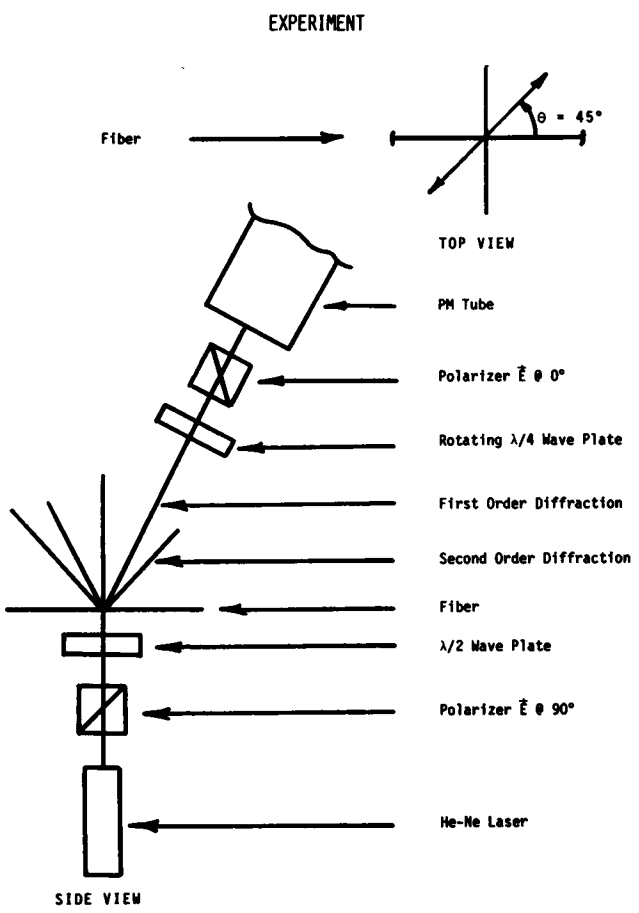

FIGURE 2 Schematic representation of the actual optical apparatus for measuring polarization properties of diffracted light.

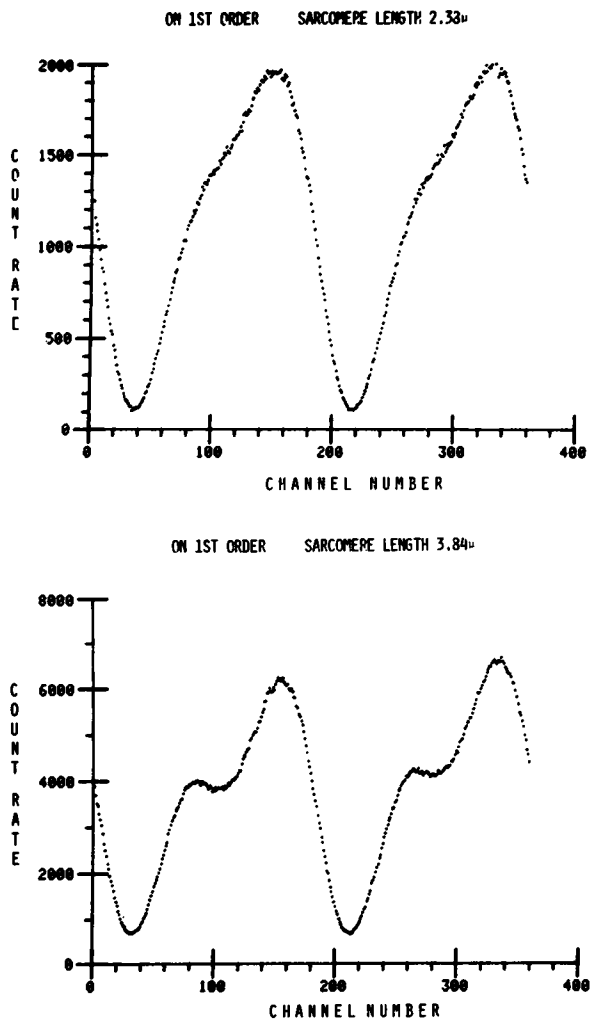

FIGURE 3 Data of I vs. Θ (Eq. 4) for first-order diffraction pattern obtained at two sarcomere lengths.

isolated it is inspected under a dissecting microscope for damage. A phase-contrast microscope at 60 power is used on a random basis to further check the quality of fibers used from time to time. At the time of inspection, the diameter is determined by using a precision Zeiss graticule (Carl Zeiss, Inc., New York, NY) and Bausch and Lomb micrometer eyepiece (Bausch and Lomb Inc., Scientific Optical Products Div., Rochester, NY). The fiber is then placed in a cooled tray of Ringer's solution and the suture connected to micromanipulators on either end of the tray.

RESULTS

All together, 38 single fibers were used in these experiments. Approximately five samples were used to perform initial calibrations. All other fibers (~30) that were examined for their optical depolarization properties exhibited very similar spectra, and we report on data from representative samples in this section.

Figs. 3 *a* and *b* show representative data taken from a single fiber experiment at two different sarcomere lengths. The vertical axis represents the intensity of light in number of counts per second, while the horizontal axis represents the angular rotation of the λ/4-wave plate in degrees. We see here that the polarization changes upon sarcomere length change. A comparison of data with the ideal representations of linearly polarized light, circularly polarized light, and arbitrary elliptically polarized light (Fig. 4) show that light from the first-order diffraction peak is indeed highly elliptically polarized. On the other hand, a signal from nonperiodic scatterers, which produce the background scattering contribution but not the sarcomere-related diffraction pattern, is far less depolarized (Fig. 5). Furthermore, as is expected from random contribution, this off-order signal is almost independent of the sarcomere length. Table I summarizes a typical data set from a representative fiber experiment. The polarization parameters are computed from initially fitting the data to Eq. 11. It is seen that δ_M (Eq. 11) exhibits a strong negative slope with passive sarcomere length increase. On the other hand, the parameter that is sensitive to intrinsic change of polarizability, α_M (Eq. 14), remains relatively constant during a given stretch and release study. Figs. 6 and 7 exhibit these trends for representative fibers. The best-fit linear curve shows that the coefficient for phase shift per length is $-12°/\mu m$ (Fig. 6), while off-axis contribution to δ_M is constant. In Fig. 7 the constancy of α_M is very evident.

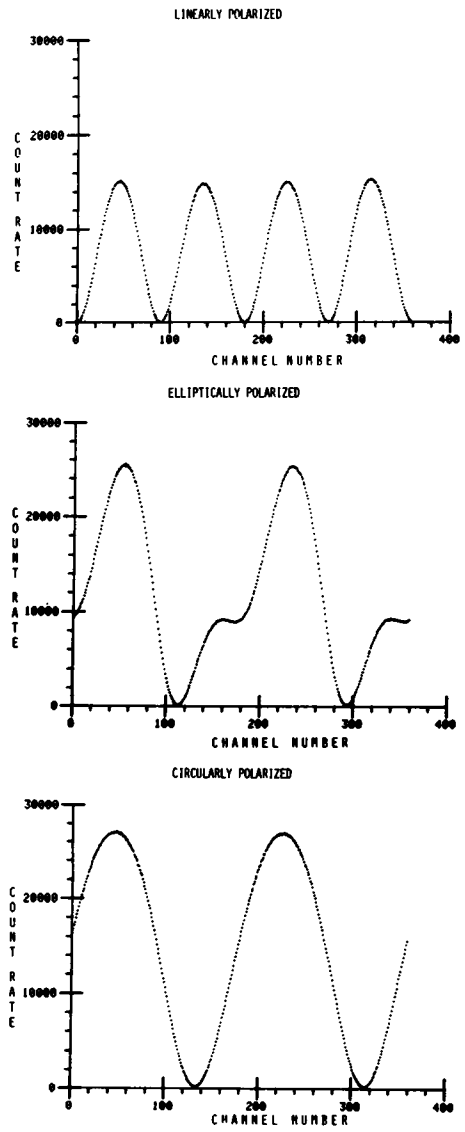

FIGURE 4 I vs. Θ data for control experiments, which are linearly polarized, arbitrary elliptically polarized, and circularly polarized light.

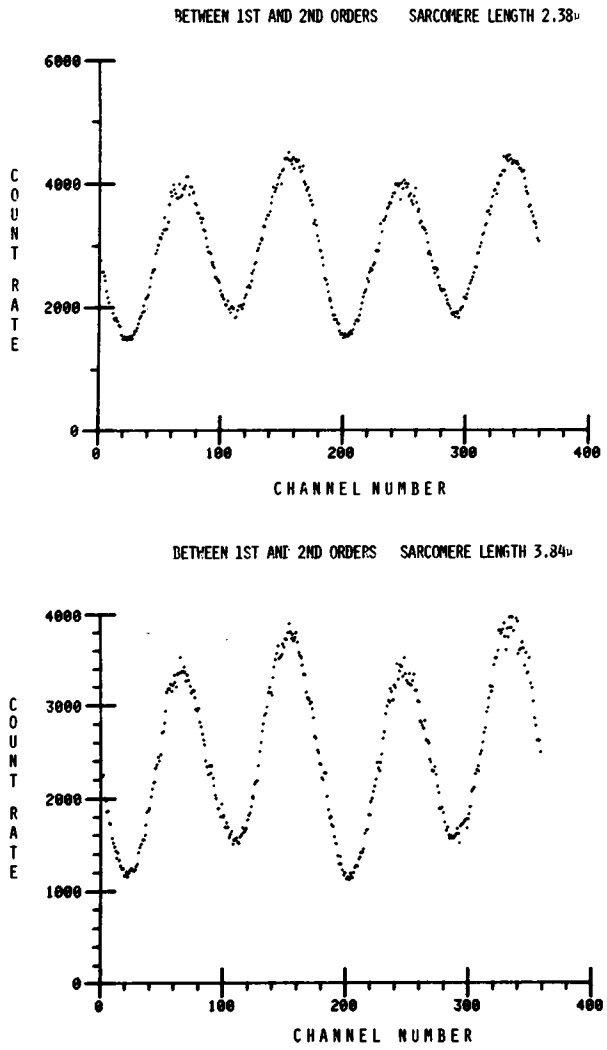

FIGURE 5 I vs. Θ for off-order scattering pattern at two different sarcomere lengths.

Data from all stretches on each of five different fibers were averaged. The variances calculated are shown by the vertical error bars. We see that fibers of various diameter, even when averaged over all stretches, give consistent α_M values to within ~10%.

DISCUSSION

Experimental and theoretical methods have been presented here to completely characterize the polarization properties of light diffracted from single fibers of skeletal muscle. Given the polarization properties of the incident light and the polarization transformation properties of optical components used to investigate diffracted light, we have shown

TABLE 1
REPRESENTATIVE DATA AND ANALYSIS PARAMETERS FOR A SINGLE STRETCH EXPERIMENT

Title	I	Q	U	V	α	δ (degrees)	χ^2	L (μm)
36 A1R	2991.62	0.1865	−0.4975	0.8178	36.7899	58.6836	1.1669	2.5138
36 B1R	4771.68	0.1735	−0.6235	0.7368	37.4170	49.7619	0.8087	2.7836
36 C1R	1421.41	0.1917	−0.6187	0.7233	36.0711	49.4594	0.5873	3.0893
36 D1R	8489.00	0.1936	−0.6617	0.6817	35.9061	45.8509	2.8103	3.3586
36 E1R	3370.52	0.1416	−0.7420	0.6013	36.3731	39.0210	0.3070	3.9158
36 F1R	3647.58	0.2070	−0.6030	0.7345	35.9320	50.6126	0.7843	2.5138

Five stretches were conducted on sample 36, looking at the first-order diffraction pattern on one side of incident beam. Fiber was returned to ~2.5 μm in run 36 F1R. I was normalized to unity before Q, U, and V were determined.

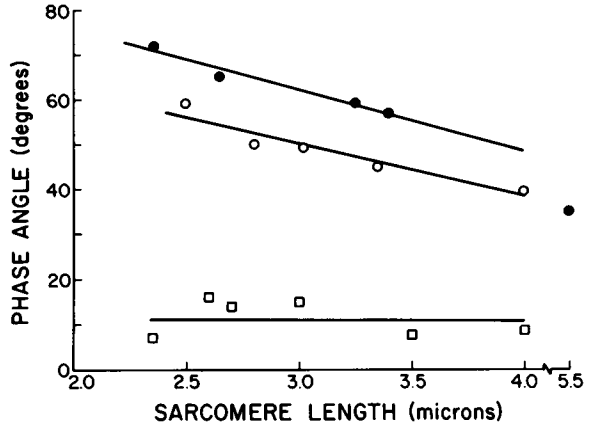

FIGURE 6 Representative phase angle (δ_M) variation vs. sarcomere length for first-order diffraction for two different fiber diameters (○, 53 μm; ●, 60 μm) and for off-order scattering, □.

that there is a unique characterization of the optical polarization properties of a single fiber. Specifically, both $\mathbf{V}_M$ and $\bar{\bar{M}}_M$ (Theory section) can be determined for each specified condition of the fiber. From the present studies on passively stretched fibers, we presented three major new findings.

(*a*) The extent of depolarization of incident light is greater on the peaks of the diffraction order than off the diffraction orders. Because observed diffraction phenomenon depends upon the presence of arrays of material that exhibit very specific index of refraction periodicity, these observations indicate that indeed it is the periodic arrays that are optically anisotropic. We have shown here that the materials that do not form arrays with sarcomere periodicity are minimally anisotropic; the phase rotation from this latter case is $\sim +10°$ as opposed to $\sim +60°$ for on-order at a sarcomere length of 2.4 μm, which indicates that the periodic arrays are far more anisotropic than the remaining medium, which includes mitochondria, membraneous matter, and other randomly placed proteins.

(*b*) Through careful analysis of the data from ~30 fibers, we show that the phase shift δ_M decreases with increasing sarcomere length. This result on its own cannot

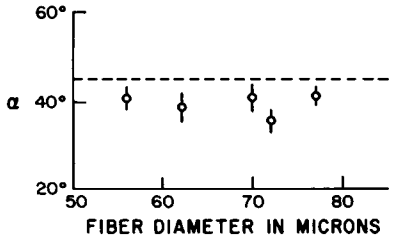

FIGURE 7 Ratio of polarizabilities as defined by Eq. 8 is plotted against fiber diameters. Each point represents the average and standard deviation of all data points from that particular fiber irrespective of the sarcomere length. The constancy of α is seen by the small standard deviation on each point. The average α value of 40° is compared with the incident polarization angle of 45°, ---.

distinguish between the various possible contributions to the phase shift because δ_M is a function of both index change between the two axes as well as the effective path length, d, and E_x, (z', t) and E_y, (z', t) are both functions of δ_M as well as α_M.

(*c*) We have, however, a measurement of α_y'/α_x' that shows that this quantity is indeed constant in the stretch experiment. The combination of these two results can be examined in the following manner: if we assume that the length variations will affect the polarizability along a particular axis according to

$$\alpha_i = \alpha_{0i} + \delta\alpha_i = [1 + R_i(L)]\,\alpha_{0i}, \qquad i = x, y, \tag{15}$$

where $R_i = \delta\alpha_i/\alpha_i$, then (for small R_i), Eq. 14 becomes

$$\delta_M(L) \approx \frac{2\pi}{\lambda} d(L) \left\{ \alpha_{0x}^{1/2} \left[1 + \frac{R_x(L)}{2} \right] - \alpha_{0y}^{1/2} \left[1 + \frac{R_y(L)}{2} \right] \right\}, \tag{16}$$

while

$$\tan \alpha_M(L) \approx \frac{\alpha_{0y}}{\alpha_{0x}} \{1 + [R_y(L) - R_x(L)] - R_x R_y\}. \tag{17}$$

We see that the experimental results of α_M being constant, while $\delta(L)$ changes can come about in only two situations: (*a*) $R_x = R_y = 0$, when all of the phase contribution comes from $d(L)$, and when (*b*) $R_x = R_y \neq 0$, but R_x and R_y are small. In this case, $\tan \alpha_M$ has only second-order dependence in the product of $R_x R_y \approx R^2$, whereas $\delta(L)$ has first-order dependence on R_y and R_x.

For all cases where $R_x \neq R_y$, one sees that Eqs. 16 and 17 will both exhibit first-order variations upon length changes. As shown in Fig. 7, we have not observed any appreciable L dependence in α_M. Thus we do not believe there are anomalously large fluctuations in $\delta\alpha_x$ or $\delta\alpha_y$.

We next must rule out the possible contributions to the observed result from possible alternative phenomena. (*a*) The simple stretching of a constant volume element will indeed decrease the radial dimension and therefore d of Eq. 14. Since Rome (15) has shown sarcomere volume to be constant to good approximation, then $d = 2(V/\pi L)^{1/2}$. Differentiating Eq. 14 with respect to L leads to

$$\frac{d\delta}{dL} = -\frac{2\pi}{\lambda_0} \left(\frac{V}{\pi} \right)^{1/2} (\alpha_x^{1/2} - \alpha_y^{1/2}) \frac{1}{L^{3/2}}. \tag{18}$$

One sees that a negative slope is expected for the situation presented here, $|\alpha_x| > |\alpha_y|$. However, this simple prediction is nonselective with respect to the sarcomere periodicity. In our experiment, the nonselective component is the off-order scattering contribution. That component is only minimally depolarized and exhibits imperceptible length-induced changes. We therefore can conclude that the variation of traversal distance, d, cannot explain our on-order depolarization effects.

(*b*) The generally accepted version of what constitutes form birefringence may be found in Born and Wolf (16). If one imagines a bundle of glass rods arranged into a large

cylindrical column, and if one allows a small space between rods, then the cross-sectional view perpendicular to the axis of this cylinder is a circle with many small circles within. An electric field **E**, which has a component along the transverse direction, will experience an averaged dielectric constant that is a composite value of the glass rods and the medium in between. The electric field parallel to the rod axes, however, experiences an averaged dielectric constant that is a composite value of the glass rods and the medium in between. The electric field parallel to the rod axes, however, experience a different nonaveraged index of refraction. Thus even if the rods were isotropic, the imposed boundary conditions will create optical depolarization for a transmitted beam of light that was initially polarized. This effect is a function of the volume fraction of either components where the rods and the medium must have alternate spacings that are comparable to or less than the wavelength of light. Wiener (17) originally derived an expression to quantify the birefringence effect due to this arrangement of isotropic elements. In the work of Taylor (8), muscle fiber diameter was changed through variation of the ionic strength of the Ringer's solution. A 2% decrease in fiber diameter led to ~4% increase in form birefringence according to experiment and Wiener's theory. For the stretch experiments conducted here, the fiber length was increased from 2.4 to 3.8 μm. This ~50% increase in length translates to ~25% decrease in diameter. According to the Wiener theory, ~50% increase in form birefringence can be expected just due to stretch. Two factors argue against form birefringence affecting our results. First of all, we have not seen such a 50% increase in the change in δ upon stretch, either on- or off-diffraction order. The second and perhaps much stronger argument against the form effects is that the form contribution, as perceived by the Wiener theory, is also independent of the axial A-I situations.

We proceed to examine a third possible cause. It has been well-established that the fast axis of the anisotropic A-band is along the direction perpendicular to the α-helix axis of the myosin bundle (18). There also is evidence that a flexible joint exists between the LMM and the S-2 segments of the myosin rod (5). If these anisotropic S-2 elements have a fixed orientation with respect to the fiber axis when they are within the overlap region, then there is a well-defined degree of anisotropy. Upon passive stretch, more and more of these elements slide out of the region where f-actin filaments are. These S-2 elements, which are free of the presence of actin, may then be freer to revolve about the LMM–S-2 hinge. In our time-averaged studies, the average depolarization experienced by the incident-light source is then decreased because the averaged slow axis now is more aligned along the light propagation direction, thus anisotropy is decreased.

In the work of Colby (19), intrinsic birefringence within the A-band was found to have increased more than simple material addition due to overlap. This nonadditive increase in birefringence has been interpreted as possible actomyosin interaction, resulting in additional intrinsic birefringence. From our result, large optical depolarization at short lengths may also be interpreted as orientational change of the S-2 within this region of overlap.

As pointed out earlier, changes in the values of polarizabilities will result in a change of α_M. This change depends strongly on the ratio of anisotropy changes R_x and R_y. We have shown that if $R_x = R_y$, then the effect of length change on α_M is second-order small, which may be too small to be clearly discerned in these experiments. The idea that phase transition within the anisotropic region could cause some of the longitudinal motion in the active muscle contractile dynamics has been proposed (20). The sensitivity of our technique to that change remains to be evaluated.

The present experiment reveals a tool that is more selective than the birefringence probe for studying muscle structure and dynamics. The complicating aspects of water contribution, membrane contribution, and other mechanically induced artifacts such as a twisted fiber (21) cannot produce a diffraction pattern that reflects the correct sarcomere length and periodicity. In conducting the experiments on the peaks of the diffraction pattern, only the specific Fourier components of those periodic elements are implicated. This observed depolarization of light is due only to optically anisotropic elements that exhibit spatial periodicity of the sarcomere.

An essential measure of the true potential of this technique is the detection of changes of optical depolarization upon activation under isometric conditions. Toward this end, preliminary experiments are being conducted to first examine the changes of optical depolarization in the rigor-relaxed transition of skinned fibers. A separate publication will discuss these results.

The authors acknowledge the skillful assistance in single fiber dissection by Ms. Martha Corcoran. Enlightening discussions with Dr. Robert Walraven on the Mueller matrix calculus is deeply appreciated. The authors also express their thanks to Professor R. J. Baskin and Dr. R. L. Lieber for stimulating discussions and critical readings of this manuscript.

We gratefully acknowledge the National Institutes of Health (grant AM26817) for their support to Y. Yeh.

Received for publication 20 May 1982 and in final form 22 November 1982.

REFERENCES

1. Cohen, C., and A. G. Szent-Gyorgi. 1957. Optical rotation and helical polypeptide chain configuration in α-proteins. *J. Am. Chem. Soc.* 79:248.
2. Harrington, W. F. 1971. A mechanochemical mechanism for muscle contraction. *Proc Natl. Acad. Sci. USA.* 68:685–689.
3. Huxley, A. F., and R. Simmons. 1971. Proposed mechanism of force generation in striated muscle. *Nature (Lond.).* 233:533–538.
4. Harvey, S., and H. Cheung. 1977. Fluorescence depolarization

studies on the flexibility of myosin rod. *Biochemistry.* 16:5181–5187.
5. Highsmith, S., C. C. Wang, K. Zero, R. Pecora, and O. Jardetzky. 1982. Bending motions and internal motions in myosin rod. *Biochemistry.* 21:1192–1197.
6. Podolsky, R. J. 1979. Dynamics. *In* Molecular Basis of Force Development in Muscle, N. B. Ingels Jr., editor. Palo Alto Med. Research Foundation, Palo Alto. 27–35.
7. Hazelgrove, J. C., and H. E. Huxley. 1973. X-ray evidence of radial cross-bridge movement and for the sliding filament model in actively contracting skeletal muscle. *J. Mol. Biol.* 77:549–568.
8. Taylor, D. L. 1976. Quantitive studies on the polarization optical properties of striated muscle. *J. Cell. Biol.* 68:497–511.
9. Weiss, R., and M. Morad. 1981. Intrinsic birefringence signal preceding the onset of contraction in heart muscle. *Science (Wash. DC).* 213:663–665.
10. Mathieu, J. P. 1975. Optics. Pergamon Press, Ltd., Oxford. Ch. 8.
11. Yeh, Y., R. J. Baskin, R. L. Lieber, and K. P. Roos. 1980. Theory of light diffraction by single skeletal muscle fibers. *Biophys. J.* 29:509–522.
12. Shurcliff, W. A. 1962. Polarized Light: Production and Use. Harvard University Press, Cambridge. Ch. 2.
13. Berne, B. J., and R. Pecora. 1976. Dynamic Light Scattering. John Wiley and Sons, Inc., New York. 33–36.
14. Bevington, P. R. 1969. Data Reduction and Error Analysis for the Physical Sciences. McGraw-Hill, Inc., New York. 232–242.
15. Rome, E. 1972. Relaxation of glycerinated muscle: low-angle x-ray diffraction studies. *J. Mol. Biol.* 65:331–345.
16. Born, M., and E. Wolf. 1965. Principles of Optics. 3rd. ed. Pergamon Press, Ltd. Oxford. 705–708.
17. Wiener, O. 1912. Die Theorie des Mischkörpers für der Fall der Stationären Strömung-I. *Die Mittel-wertzätze Math Phys.* 32:509–604.
18. Huxley, H. E., and J. Hanson. 1957. Quantitative studies on the structure of cross-striated myofibrils I. *Biochim. Biophys. Acta.* 23:229.
19. Colby, R. H. 1971. Intrinsic birefringence of glycenated myofibrils. *J. Cell Biol.* 51:763–771.
20. Julian, F. J., K. R. Sollins, and M. R. Sollins. 1974. A model for the transient and steady state mechanical behavior of contracting muscle. *Biophys. J.* 14:546–562.
21. Eberstein, A., and A. Rosenbalck. 1963. Birefringence of isolated muscle fibers in twitch and tetanus. *Acta Physiol. Scand.* 57:144–166.
22. Azzam, R. M. A., and N. M. Bashara. 1977. Ellipsometry and Polarized Light. North Holland Publishing Company, Amsterdam.